SYNOPTIC MAPS OF SOLAR WIND: COMPARISON OF IPS DATA AND THE NOAA/SEC VERSION OF THE WANG AND SHEELEY MODEL

BALA BALACHANDRAN
Instituto de Geofisica, Universiad Nacional Autónoma de México, Coyoacán, D.F. 04510 México

(Received 20 September 1999; accepted 23 March 2000)

Abstract. Since the 1970s, the Solar-Terrestrial Environment Laboratory, Japan, has been publishing synoptic maps of solar wind velocity prepared using the technique of interplanetary scintillation. These maps, known as V-maps, are useful to study the global distribution of solar wind in the heliosphere. As the Earth-orbiting satellites are unable to probe regions outside the ecliptic, it is important to exploit the scope of interplanetary scintillation to study the solar wind properties at these regions and their relation with coronal features. It has been shown by Wang and Sheeley that there exists an inverse correlation between rate of magnetic flux expansion and the solar wind velocity. The NOAA/Space Environment Center daily updated version of the Wang and Sheeley model has been used to produce synoptic maps of solar wind velocity and magnetic field polarity for individual Carrington rotations. The predictions of the model at 1 AU have been found to be in good agreement with the observed values of the same. The present work is a comparison of the synoptic maps on the source surface using the interplanetary scintillation measurements from Japan and the NOAA/SEC version of the Wang and Sheeley model. The two results agree near the equatorial regions and the slow solar wind locations are consistent most of the times. However, at higher latitudes within $\pm 60^\circ$, the wind velocities differ considerably. In the Wang and Sheeley model the highest speed obtained is $\sim$ 600 km s^{-1} whereas in the IPS results velocities as high as 800 km s^{-1} have been detected. The paper discusses the possible causes for this discrepancy and suggestion to improve the agreement between the two results.

1. Introduction

Ever since the first spacecraft detected solar plasma in the interplanetary medium, the solar wind and the heliospheric magnetic field have been studied extensively leading to several important results and discoveries. However, Earth-orbiting spacecraft are limited to $\pm 7.25^\circ$ near the solar equator. There were several outer planet missions like *Pioneer* and *Voyager* attaining latitudes as high as 30° but they were all at heliocentric distances of 5 AU or beyond where the solar wind is highly evolved. *Ulysses*, on the other hand, due to its high orbital inclination, returned inward to about 1.3 AU at perihelion and circled the Sun passing both the poles at $\pm 80^\circ$. This polar pass of *Ulysses* is known as the 'fast latitude scan' and made the in situ measurements of solar wind plasma in these regions for the first time. However, launching satellites like *Ulysses* is very rare and so, the properties of out-of-ecliptic solar wind remain unexplored. One way to probe these regions is to employ remote sensing techniques such as interplanetary scintillation (IPS) or

Solar Physics **195:** 195–208, 2000.

comet observation. The latter is rather infrequent, whereas using the former one can probe out-of-ecliptic solar wind all the time within 1 AU (Hewish, Scott, and Willis, 1964; Kakinuma, Washimi and Kojima, 1973; Coles *et al.*, 1978). With an appropriate choice of the frequency of observation, IPS can give information about the solar wind very close to the Sun as well. Therefore, IPS, though indirect, provides a rather unique way of obtaining information about the solar wind at all latitudes within 1 AU and at all times.

Interplanetary scintillation is analogous to optical twinkling of stars, scaled to radio frequencies. Radio signals from compact radio sources such as pulsars are modulated by the irregularities in the solar wind. The scattered radio waves interfere with each other as they propagate to the Earth forming a diffraction pattern that drifts across the observer's plane with solar wind speed. A set of suitably spaced radio receivers on Earth detect these diffraction patterns with a time lag. A cross-correlation analysis of signals between pairs of antennae gives the velocity of the diffraction pattern. This velocity is assumed to be the solar wind velocity at the point of closest approach to the Sun (P-point) of the line-of-sight to the scintillating radio source. The P-point approximation has been shown to be nearly valid for most observations beyond 0.5 AU, especially for the slow solar wind (Watanabe and Kakinuma, 1972; Coles *et al.*, 1978; Coles and Kaufman, 1978).

The solar wind velocity V_R estimated by IPS at various distances in the heliosphere is projected back to the source surface (situated at a distance of 2.5 $R_\odot$ from the center of the Sun, within which all the magnetic field is assumed to be derived from a potential and there is no current; at the source surface, all the fields are radial) along the Archimedean spiral using the relations

$$\Phi_0 = \Phi_R + \frac{R\Omega}{V_R}, \qquad \Theta_0 = \Theta_R \,, \tag{1}$$

where, Φ_0 and Φ_R are the longitudes, and Θ_0 and Θ_R the latitudes, on the source surface and at a distance R from the Sun, respectively. Ω is the angular speed of solar rotation. These velocities are then used to make a synoptic map (V-map) in Carrington longitude and heliographic latitude. However, the source surface is situated within the acceleration region of the solar wind. Therefore, the application of Equations (1) all the way to the source surface could be misleading.

Wang and Sheeley (1990) obtained a statistically significant inverse correlation between the solar wind velocity and the rate of expansion of magnetic flux. That is, fast solar wind originates from regions with small magnetic divergence whereas slow solar wind emanates from regions where the magnetic divergence is high. The former corresponds to central regions of coronal holes, while the latter corresponds to the boundaries of open field regions overlying closed field regions. For details of the results and the physical basis for the relationship refer to Wang and Sheeley (1991) and Wang (1993). At the NOAA Space Environment Centre (NOAA/SEC), Boulder, a modified version of Wang and Sheeley model has been used to make synoptic maps similar to the V-maps from IPS observations and to predict the

velocity and magnetic field polarity at 1 AU. The present paper is a comparative study of the results obtained by the two methods.

2. Data and the Preparation of V-maps

Using their multi-station IPS facility, the Solar–Terrestrial Environment Laboratory (STELab), Nagoya University, Japan, has been preparing and publishing V-maps since the 1970s. These maps are useful in studying the global structure, distribution and evolution of solar wind in the heliosphere. Recently, using the Wang and Sheeley model, Arge and Pizzo (1998) have obtained similar maps, making use of the relation between magnetic flux expansion factor and velocity of solar wind. The data used in the present study is as follows: Carrington rotations CR 1894–1896 cover a period from 23 March to 12 June, 1995; CRs 1898–1900, from 10 July to 29 September, 1995 and CR 1925–1927 include the period from 15 July–5 October, 1997. The data for these V-maps were superposed over three Carrington rotations indicated in each set. The V-maps computed using IPS measurements as well as Wang and Sheeley model for these periods are shown in Figures 1, 2, and 4. Since the period of study was near solar minimum, very little evolution of solar wind was expected from one rotation to the next and most of the long-lived, large-scale structures were assumed to be retained. Due to many reasons, the velocities beyond $\pm 60^\circ$ may not be reliable and therefore, excluded from the present study. The location of the coronal holes on the source surface and the footpoints mapped on the photosphere using the potential field model of Hoeksema (for the Carrington rotation CR 1898) is depicted in Figure 3. The computation includes all the multi-poles up to order 9.

In the following subsections, the two methods are described in some detail and the latitudinal profile obtained from these V-maps is introduced. A detailed discussion of the results is presented in Section 3.

2.1. Predicted V-maps of NOAA/SEC using Modified Wang and Sheeley model

The rate at which the flux tube expands in solid angle between the photosphere and the source surface can be represented mathematically as

$$f_s = \left(\frac{R_\odot}{R_{ss}}\right)^2 \frac{B_r(\text{phot})}{B_r(ss)}\,, \tag{2}$$

where $B_r(\text{phot})$ and $B_r(ss)$ are the radial components of magnetic fields at the photosphere and the source surface, and $R_\odot$ and $R_{ss} = 2.5\ R_\odot$ are the photospheric and source-surface radii, respectively. Wang and Sheeley (1990, 1994) found that the computed values of f_s were associated with different ranges of solar wind speed at 1 AU. However, Arge and Pizzo (1999) obtained the following relation between the flux expansion factor and the solar wind velocity by iteration:

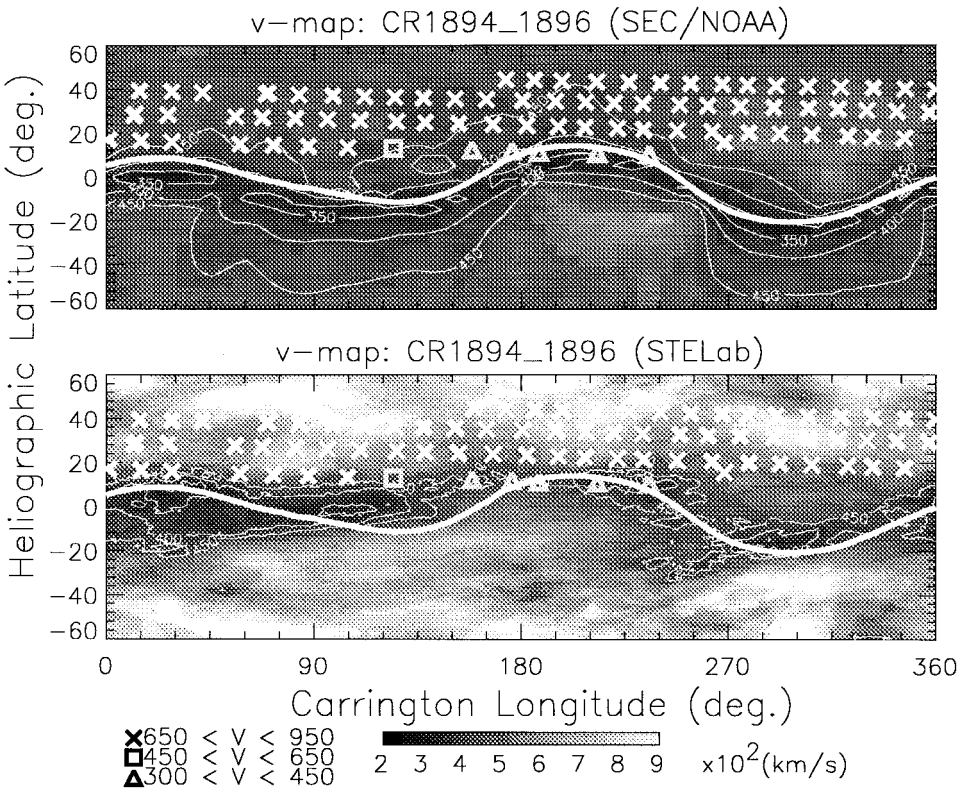

Figure 1. The V-map for superposed CRs 1894–1896 (1995). The upper panel is the predicted V-map of NOAA/SEC using the Wang and Sheeley model while the lower panel is the V-map obtained at STELab, Japan, using IPS data. The thick white solid line is the magnetic neutral line for CR1894. The thin white contours represent the slow solar wind ($V \leq 450$ km s^{-1}) plotted at an interval of 50 km s^{-1}. The *Ulysses* data projected back to the source surface during the same period is over-plotted with various symbols.

$$V_{sw} = 267.5 + 410.0/f_s^{(1.0/2.5)} \tag{3}$$

where, V_{sw} is the speed of the solar wind and f_s is the flux expansion factor obtained using Equation (2). At NOAA/SEC, the Wang and Sheeley model has been updated using the daily magnetograms from the Wilcox Solar Observatory and used to obtain V-maps and magnetic field polarity (http://sec.noaa.gov/∼narge/). The velocity, calculated according to Equation (3), and the magnetic field polarity predicted by the model at 1 AU were found to be in good agreement with the *in situ* measurements (Arge and Pizzo, 1998).

The V-maps prepared using the NOAA/SEC version of the Wang and Sheeley model and Equation (3) for Carrington rotations 1894–1896 and 1898–1900 (1995) and 1925–1927 (1997) are depicted in the upper panels in Figures 1, 2, and 4. Superposed is the magnetic neutral line obtained from the potential field model of Hakamada, obtained at STELab, (thick white line), for CR 1894 in Fig-

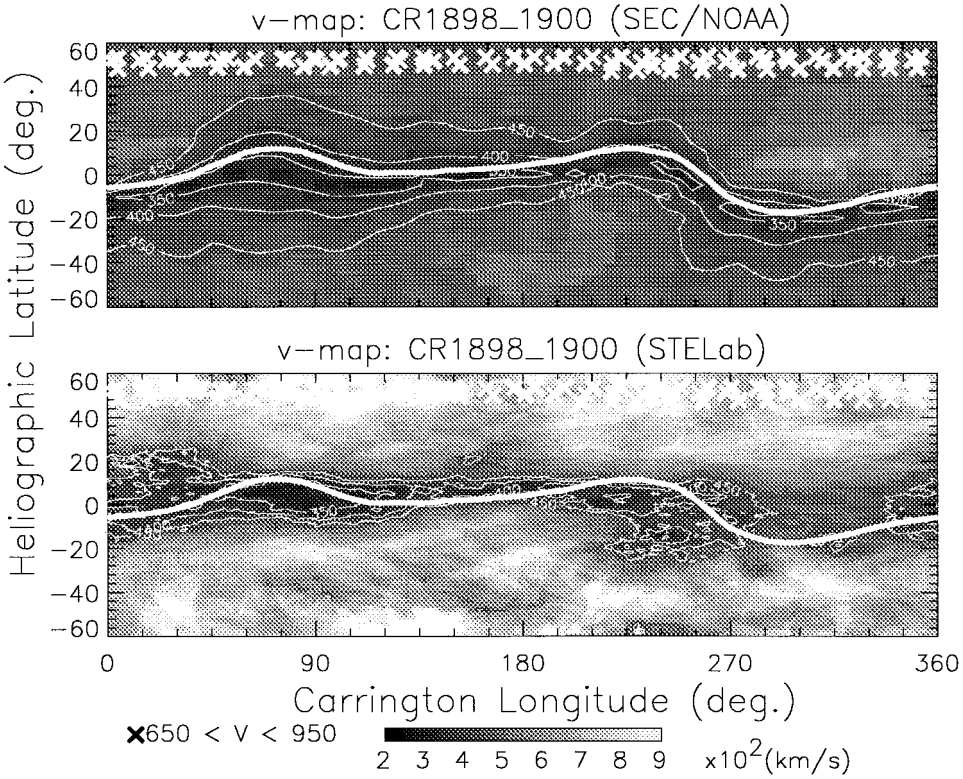

Figure 2. The same as Figure 1 but for CRs 1898–1900 (1995). The neutral line is for CR 1898.

ure 1, CR 1898 in Figure 2, and CR 1925 in Figure 4, respectively. The thin white lines are contours of velocities $\leq$ 450 km s^{-1} and are plotted at intervals of 50 km s^{-1}. The symbols represent the velocities observed by *Ulysses* during the same period beyond the Earth's orbit (between about 1.35 and 1.75 AU), projected back to the source surface, using Equation (1). Different ranges of velocities are depicted by different symbols: triangles are $300 < V < 450$ km s^{-1}, squares are $450 < V < 950$ km s^{-1} and crosses are $650 < V < 950$ km s^{-1}.

2.2. SYNOPTIC MAPS USING IPS DATA

The IPS facility at STELab consists of four stations, operating at a frequency of 327 MHz (Asai *et al*., 1995). It is capable of observing about 30 radio sources daily and employs the technique of cross-correlation between pairs of antennae to obtain the solar wind speed. In the technique of IPS, the solar wind velocity is measured as an integration of all the speeds along the line-of-sight to the radio source, weighted by the distribution of density fluctuation. Therefore, the velocity is biased and is different from the real velocity at P-point. Applying the technique of Computer Assisted Tomography (CAT), the bias caused by the line-of-sight in-

tegration can be minimized as has already been shown by its application to the IPS data from STELab (Jackson *et al*., 1988; Kojima *et al*., 1998). For the application of tomography, both the solar wind velocity and the density fluctuation are necessary. In the present study, the latter is assumed to have a power-law dependence on the former, of the form

$$\delta N_e(z) = V^{-\gamma}(z) \; . \tag{4}$$

Following the studies by Kakinuma, Washimi, and Kojima (1982) on the speed dependence of the density fluctuations, a value of 0.5 has been chosen for γ. For the successful application of tomography, a large number of data points ($\sim$500) per Carrington rotation is necessary. During the period chosen for the present study, the data was insufficient to make V-maps for individual Carrington rotations and hence the data over three rotations were superposed. Since the periods of study (1995, 1997) are near solar minimum, very little evolution of solar wind was expected from one rotation to the next and most of the long-lived, large-scale structures were assumed to be retained. The V-maps obtained for Carrington rotations CRs 1894 –1896, CRs 1898–1900 and CRs 1925–1927 are presented in the lower panels in Figures 1, 2, and 4. Also, the source surface magnetic neutral line (thick white solid line) and velocity contours (thin white lines), as in the upper panel, are over-plotted. The crosses in Figure 2 represent the velocities detected by Ulysses during the same period, in the range $650 \leq V \leq 950$ km s^{-1}. Due to certain technical problems, the *Ulysses* data for CRs 1925–1927 could not be plotted.

2.3. LATITUDINAL PROFILE

In a study using IPS data for 15 years, Rickett and Coles (1991) showed that the yearly averaged solar wind velocity increases sharply with heliographic latitude during low and declining phases of solar activity whereas the velocity remains uniformly low at solar maximum. A careful analysis of the V-maps published by the IPS group at STELab, Japan, reveals the same tendency. That is, the sharp latitudinal gradient of velocity observed during quiet periods is no longer there during disturbed periods when the slow and fast winds are randomly distributed in the heliosphere (Kojima and Kakinuma, 1990).

Figures 5–7 depict the latitudinal profiles of solar wind velocity obtained from the IPS measurements (solid line) and the modified Wang and Sheeley model (dashed line), for the same rotations shown in Figures 1, 2, and 4. The data for these figures were averaged over the entire longitude range. The curve from the IPS data is consistent with the earlier works of Rickett and Coles but that from Wang and Sheeley model is far from agreement. This (dashed line) resembles an active period of the Sun. The difference between the two curves are very significant and suggests the limitation of the Wang and Sheeley model in handling the high latitudes.

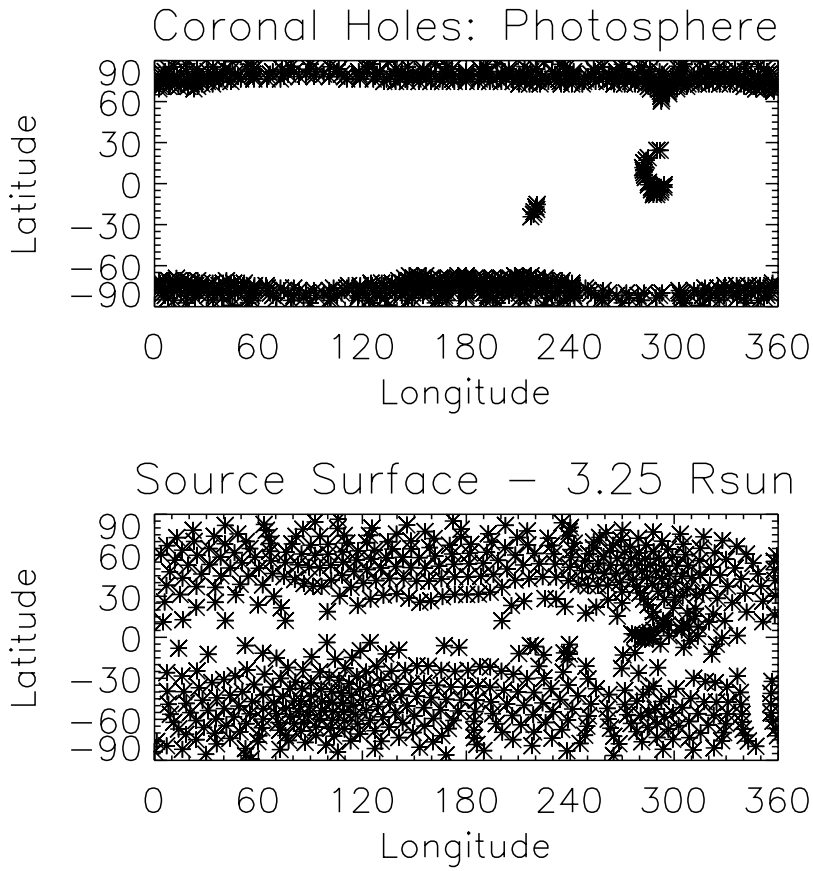

Figure 3. The location of coronal holes mapped on the photosphere (*upper panel*) and on the source surface (*lower panel*) using the potential field model of Hoeksema, for the Carrington rotation CR 1898. This rotation corresponds to that in Figure 2. The symbols represent the location of the open field lines on the photosphere and the source surface in the upper and lower panels, respectively.

3. Discussion of the Results

The solar wind in the heliosphere has two distinct components, the slow and the fast. The former has typical velocities less than or equal to 450 km s^{-1} while the velocities of the latter is typically 500 km s^{-1} and higher. The high-speed solar wind originates from open magnetic field regions in the corona, known as coronal holes and is rather steady. On the other hand, the slow solar wind, originating from regions above the closed magnetic fields, like helmet streamers, is highly structured and evolves significantly from rotation to rotation, making it an interesting and important feature to pursue. The presence of the slow and fast components of the solar wind is very striking in the IPS results (lower panel), whereas the high-speed component in the range 650 to 850 km s^{-1} is missing in the Wang and Sheeley model of NOAA/SEC (upper panel). Also, the latitudinal width of the slow solar

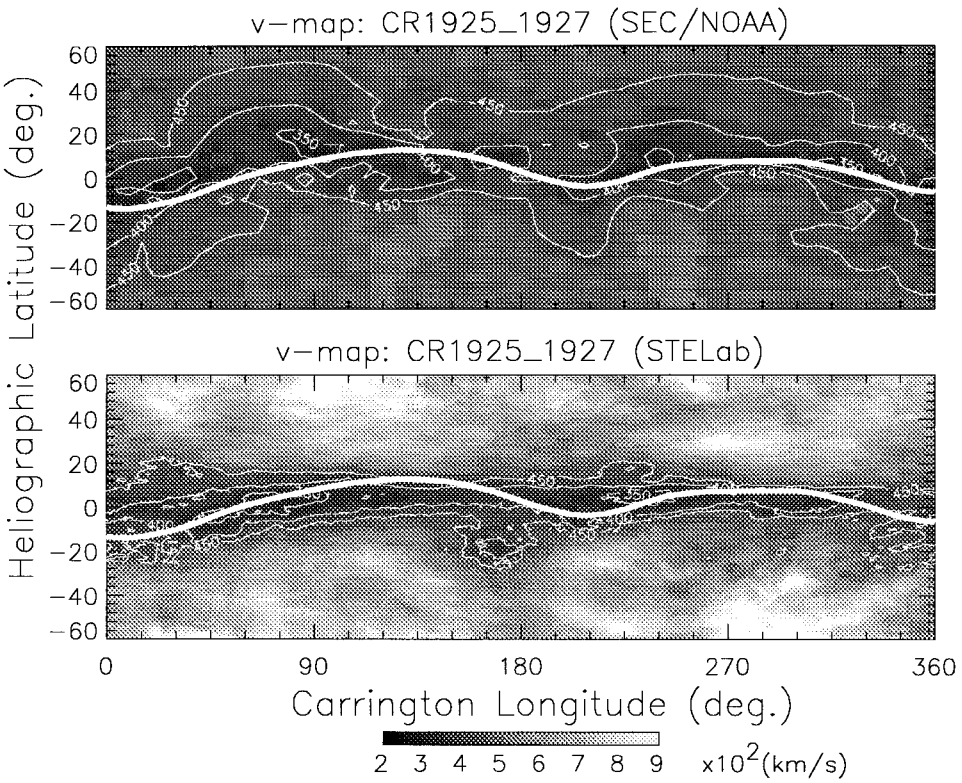

Figure 4. The same as Figure 1 but for CRs 1925−1927 (1997). The neutral line is for CR 1925.

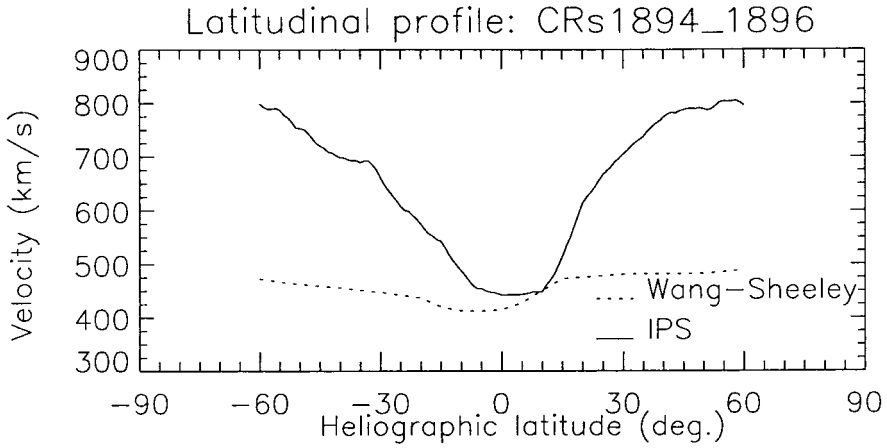

Figure 5. The latitudinal profiles of the solar wind velocity on the source surface averaged over the entire longitude. The solid line represents the IPS measurements and the dashed line, the NOAA/SEC version of Wang and Sheeley model.

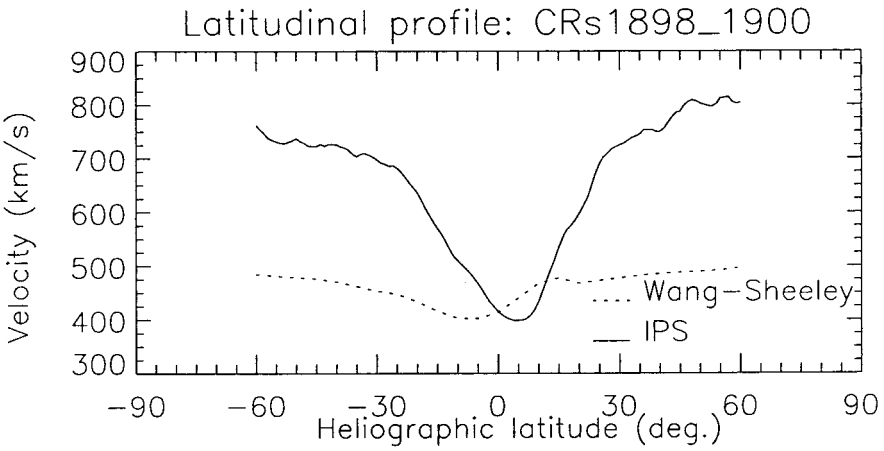

Figure 6. The same as Figure 5 but for CRs 1898–1900.

wind belt is somewhat larger in the Wang and Sheeley model of NOAA/SEC than in the IPS results. However, the longitudinal locations of the slow solar wind in the two V-maps coincide almost everywhere, except in the 90–130° longitude in Figure 1; at this region, the slow solar wind is located below the neutral line in the Wang and Sheeley model while in the IPS results they are above the neutral line. This general agreement in the longitudinal locations of the slow solar wind in both the V-maps somewhat contradicts the conclusions in Wang *et al*. (1997) where they have pointed out that their model predicts too much fast wind. However, they have also pointed out that this could be corrected for by allowing streams to interact in the model. The results shown in this paper are from the NOAA/SEC version of Wang and Sheeley model, where they have devised a simple method to include the stream–stream interaction (Arge and Pizzo, 1999).

On an average, the slow solar wind is confined within ±20° in all three Figures 1, 2 and 4, which is a little larger than the slow solar wind belt observed by *Ulysses* at about 1.34 AU: ±18° (Phillips *et al*., 1995), This seems to be consistent with other observations where the width of a streamer belt on the solar surface appeared to have a latitudinal width of about 60°, narrowed down to about 45° at 1.74 $R_{\odot}$ when observed by *Yohkoh* as well as Mauna Loa coronameter (Gosling *et al*., 1995). That is, the width of the slow speed has possibly reduced from the source surface to 1.34 AU at the time of *Ulysses* observation.

In the Wang and Sheeley model of NOAA/SEC (upper panels in Figures 1 and 2) the slow solar wind is a thin, wavy band near the solar equator and is one, single, continuous belt. During CRs 1894–96 (Figure 1), the slow-wind belt appears to be sinusoidal while during CRs 1898–1900 (Figure 2), it is parallel to the solar equator except in the longitudinal range 240–360°, where it appears to be pushed to the higher southern latitudes by fast wind from the north. Also, in Figure 2, in the longitude band 30–90°, the slow solar wind is broader in latitude than in

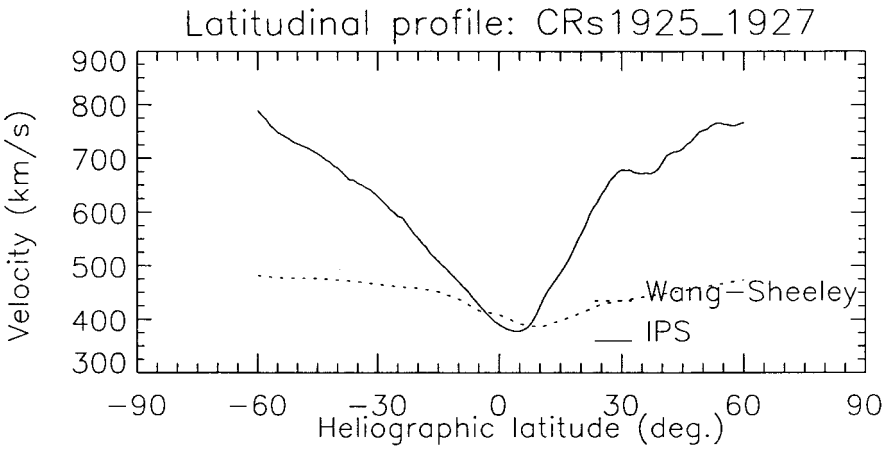

Figure 7. The same as Figure 5 but for CRs 1925–1927.

Figure 1. All these features are contrary to what is seen in the IPS results – lower panels in Figures 1 and 2. Here, the slow solar wind appears as disjoint regions near the solar equator, the region in between being occupied by high-speed wind ($\sim$ 550 km s^{-1}). In the lower panel (IPS) in Figure 2, a high-speed stream is seen to be crossing the equator near the longitude $\sim$ 280–320°. Note that at the same longitude in the upper panel (Wang and Sheeley model of NOAA/SEC), the slow-wind belt is being pushed to higher southern latitudes. From Figure 3, it is clear that there exists a coronal hole at nearly the same longitude near the equator which could be the source of the fast stream that crossed the equator in Figure 2. Figure 3 is obtained using the potential field model of Hoeksema and it is rather surprising to see the absence of a high stream crossing the equator at this location in the Wang and Sheeley model of NOAA/SEC.

In Figure 4, the slow solar wind belt is rather disjoint at a couple of places near the equator in the Wang and Sheeley model of NOAA/SEC, different from the previous two data sets, indicating an evolution of the slow solar wind with solar activity. Surprisingly, this is absent in the IPS results and the slow-wind belt is rather parallel to the equator and continuous. Also, the slow solar wind has a slightly larger latitudinal extent in the upper panel, as indicated by the velocity contours. As in the previous figures, the high latitude fast streams are absent in the Wang and Sheeley model.

Figures 5–7, the latitudinal profile of solar wind velocity, show the striking difference between the two V-maps. Note that there is no fast wind at high latitudes with velocities greater than 500 km s^{-1} in the NOAA/SEC version of Wang and Sheeley model (dotted line). Here, the curve is rather flat with a small dip near the equator. Also, there is a marked north-south asymmetry in all the figures. At the same time, the IPS results show sharp velocity gradients, consistent with previous results (Rickett and Coles, 1991). The period of study, *viz* the years 1995 and 1997,

is one with low activity, and so, the latitudinal profile is expected to be as sharp as the IPS results. The trend seen in the Wang and Sheeley model is in contrast to the *Ulysses* observations as well. During its fast latitude scan, *Ulysses* observed velocities as high as 850 km s^{-1} (excluding CMEs) at around 60° latitude in both the hemispheres, but at a heliocentric distance of $\sim$ 1.5 AU (Phillips *et al.*, 1995), which are represented by crosses in Figures 1 and 2. It also observed a belt of slow solar wind within a range of $\pm 18°$. And, in general, the wind speed exhibited a positive latitudinal gradient away from the solar equator in either hemisphere, consistent with the earlier studies (Rickett and Coles, 1991).

In short, the predicted V-map of NOAA/SEC does not agree very well with either the IPS measurements or the Ulysses observations at latitudes higher than ± 30 or 35°. The possible causes of this discrepancy are discussed in the following section.

4. Concluding Remarks

The immediate conclusion from Figures 1–7 is that the two V-maps are very much in agreement with each other near the solar equator. This is consistent with an earlier study of Arge and Pizzo (1998), where they have shown that the solar wind speed and the magnetic field at 1 AU predicted by the NOAA/SEC version of the Wang and Sheeley model was in agreement, in general, with the spacecraft observations. However, there is a large discrepancy at the higher latitudes, indicating that the model has difficulties in handling the regions where the magnetic field is predominantly open. However, this need not strictly be the implication as there are other possibilities that could be the cause of the observed discrepancy. At various stages of data analysis as well as modeling, a few important physical aspects were overlooked or ignored as a first approximation, which could introduce some errors in the final results. Below is a list of them with a brief elaboration on each.

1. The absence of heliospheric current sheet (HCS) in the Wang and Sheeley model.

As pointed out by Wang and Sheeley (1994), the potential field source surface model does not include the effect of heliospheric current sheet and therefore, the expansion of the magnetic flux tube in the region $R \geq R_{ss}$ is not correctly represented by the model. This, the omission of the current sheet, introduces some uncertainties in the latitudinal and longitudinal positions of the flux tubes for $R \geq R_{ss}$ and in turn, in the locations of the predicted wind streams. How the absence/presence of a current sheet is going to affect the high velocity distribution and even the very values of them at high latitudes needs to be tested.

2. The bias in the estimation of solar wind velocity from IPS.

In the technique of IPS, the solar wind velocity is obtained as an integration of all the velocities along the line of sight to the radio source, perpendicular to it. This includes contribution from faster and slower streams than the one crossing the P-point and causes an underestimation of the solar wind speed at low latitudes and an overestimation at higher latitudes (Kojima *et al*., 1998). However, the *Ulysses* observation of velocities as high as 850 km s^{-1} at high latitudes substantiates the IPS values. Moreover, the bias caused by the line-of-sight integration is reduced to a large extent by the application of tomography.

3. The inadequacy of the technique of inverse mapping of the velocity to the source surface.

To prepare the V-maps of solar wind on the source surface, the velocities estimated by IPS between 0.1 and 0.9 AU are mapped back using Equation (1). There are three important aspects that are neglected here: first of all, it assumes little latitudinal variation during the outward propagation of the solar wind. That is, the plasma flow is taken to be radial and all non-radial components are neglected. However, this is not strictly true as is evident in the recent LASCO coronagraphic observations of helmet streamers, which are non-radial (see, for example, January 1997, Data: High Altitude Observatory/NCAR). In such cases, a radial inverse mapping would definitely lead to a wrong location as the origin of these plasma streams. Second, the interaction between fast and slow streams is totally neglected. The velocities estimated by IPS are the resultant of, perhaps, the interaction of fast and slow streams, though such interactions within 1 AU are infrequent. In such cases, it is not easy to de-convolve the true velocity and to trace back to the real source on the corona. Finally, the very location of the source surface: at 2.5 $R_{\odot}$. This region is well within the sonic point (where the solar wind attains the supersonic value) within which the heliocentric distance dependence of the acceleration of both fast and slow wind are still not well understood. The relation is certainly different from that governed by Equation (1) and the application of it will introduce considerable uncertainty.

The non-radial nature of plasma emission and stream-stream interaction are more of a local nature, as they are infrequent in their occurrence, still not negligible. On the other hand, the inverse mapping in the region within 30 $R_{\odot}$ deserves special attention since it is a global problem being important to the spacecraft data as well. The *Ulysses* data (obtained beyond 1 AU) shown in Figures 1 and 2 were projected onto the source surface using the same relation Equation (1). That is why, perhaps, IPS data is in better agreement with the *Ulysses* data than the Wang and Sheeley model, which, of course, reassures the credibility of the IPS data. As mentioned previously, IPS is a powerful technique in inferring the solar wind properties at all

latitudes in the heliosphere and at all times. Therefore, it is important to exploit the possibilities of IPS more effectively.

In the wake of the above discussion, it appears that the major source of error could be the inverse mapping. Perhaps, it is not possible to have velocities as high as 800 km s^{-1} on the source surface, as predicted by the NOAA/SEC version of Wang and Sheeley model. The high velocities present in the IPS data could be an artifact of the 'wrong' inverse mapping from say, a region of 30 $R_\odot$, to the source surface. The IPS V-map in the present form could be valid only outside 0.3 AU or so, and not at a region so close to the Sun as the source surface. In other words, instead of taking all the way back to the source surface, the IPS V-maps should have been prepared at a distance of about 60 or 100 $R_\odot$ so as to provide a more realistic picture of the global structure of solar wind. Proceeding further backwards using Equation (1) may take the solar wind not to the source surface but, perhaps, somewhere deeper within. Though Wang and Sheeley model of NOAA/SEC has certain limitations of its own, the results are more acceptable than the IPS results as the velocities are unlikely to be the same within the sonic point as outside. Therefore, at this point, the present discussion is concluded by emphasizing the importance of trying to improve the inverse mapping technique, especially that inside a region of say, 30 $R_\odot$, so as to be consistent with the acceleration of solar wind in this region.

Acknowledgements

The author is deeply indebted to Drs V. J. Pizzo and C. N. Arge, NOAA/SEC, Boulder, USA, for kindly providing her with the results of their Wang and Sheeley model and the many discussions. She also wishes to thank Prof. M. Kojima for the IPS and magnetic neutral line data. Drs J. Burkepile and T. E. Holzer, are acknowledged for many discussions at HAO, Boulder, Colorado. Thanks are also due to Dr Silvia Bravo, UNAM, México.

Wilcox Solar Observatory data used in this study was obtained via the web site http://quake.stanford.edu/wso/ by courtesy of J. T. Hoeksema.

References

Arge, C. N. and Pizzo, V. J.: 1998, in S. R. Habbal, R. Esser, J. V. Hollweg and P. A. Isenberg (eds.), *Solar Wind 9, Proceedings of the 9th International Solar Wind Conference*, Nantucket Island, Massachusetts, U.S.A., 5–9 October 1998, p. 569.

Arge, C. N. and Pizzo, V. J.: 1999, *J. Geophys Res.*, in press.

Asai, K., Ishida, Y., Kojima, M., Maruyama, K., Misawa, H., and Yoshimi, N.: 1995, *J. Geophys. Res.* **47**, 1107.

Coles, W. A. and Kaufman, J. J.: 1978, *Radio Sci.*. **13**, 591.

Coles, W. A., Harmon, J. K., Lazarus, A. J., and Sullivan, J. D.: 1978, *J. Geophys. Res.* **83**, 3337.

Dennison, P. A. and Hewish, A. A.: 1967, *Nature* **213**, 343.
Gosling, J. T., Bame, S. J., Feldman, W. C., McComas, D. J., Phillips, J. L., Goldstein, B., Neugebauer, M., Burkepile, J., Hundhausen, A. J., and Acton, L.: 1995, *Geophys. Res. Lett.* **22** 3329.
Hewish, A., Scott, P. F., and Willis, D.: 1964, *Nature* **203**, 1214.
Jackson, B. V., Hick, P. L., Kojima, M., and Yokobe, A.: 1998, *J. Geophys. Res.* **103**, 12049.
Kakinuma, T., Washimi, H. and Kojima, M.: 1973, *Publ. Astron. Soc. Japan* **25**, 271.
Kakinuma, T., Washimi, H., and Kojima, M.: 1982, in M. A. Shea *et al*., *Proc. of the ISTP Symposium on Solar Radio Astronomy, Interplanetary Scintillation and Coordination with Spacecraft*, Spec. Rep. 233, p. 153, Air Force Geophys. Lab. Hanscom, Air Force Base Mass.
Kojima, M. and Kakinuma, T.: 1990, *J. Geophys. Res.* **92**, 7269.
Kojima, M., Tokumaru, M., Watanabe, H., Yokobe, A., Asai, K., Jackson, B. V., and Hick, P. L.: 1998, *J. Geophys. Res.* **103**, 1981.
Phillips, J. L., Bame, S. J. Barnes, A., Barraclough, B. L., Feldman, W. C., Goldstein, B. E., Gosling, J. T., and Hoogeveen, G. W.: 1995, *Geophys. Res. Lett.* **22**, 3301.
Rickett, B. J. and Coles, W. A.: 1991, *J. Geophys. Res.* **96**, 1717.
Wang, Y.-M.: 1993, *Astrophys. J.* **410**, L123.
Wang, Y.-M. and Sheeley, N. R., Jr.: 1990, *Astrophys. J.* **355**, 726.
Wang, Y.-M. and Sheeley, N. R., Jr.: 1991, *Astrophys. J.* **372**, L45.
Wang, Y.-M. and Sheeley, N. R., Jr.: 1994, *J. Geophys. Res.* **99**, 6597.
Wang, Y. -M., Sheeley, N. R., Jr., Phillips, J. L., and Goldstein, B. E.: 1997, *Astrophys. J.* **488**, L51.
Watanabe, T. and Kakinuma, T.: 1972, *Publ. Astron. Soc. Japan* **24**, 459.